

# Inverse Stability Problem and Applications to Renewables Integration

Thanh Long Vu, Hung Dinh Nguyen, Alexandre Megretski, Jean-Jacques Slotine and Konstantin Turitsyn

**Abstract**—In modern power systems, the operating point, at which the demand and supply are balanced, continuously changes in an unpredictable way due to the natural fluctuation of loads and intermittent renewable generations increasingly installed into the system. Understanding the dynamics of power systems with varying operating point would be essential to the reliable operation of power systems, and possibly allow higher integration of renewable generations. In this letter, we formulate, for the first time, the inverse stability problem of power systems, which concerns with characterizing the region of equilibrium points (EPs) that the system can reach from a given initial state. The inverse stability is rarely addressed in control systems theory, and thus, poorly understood. Exploiting quadratic bounds of the system’s energy function, we introduce an estimate for the EP region. Also, we briefly describe three important applications of this inverse stability certificate: (i) robust stability assessment of power systems with respect to renewable generations, (ii) stability-constrained optimal power flow (sOPF), and (iii) stability-guaranteed corrective actions.

**Index Terms**—Power grids, renewable generation, transient stability, emergency control, energy function

## I. INTRODUCTION

Renewable generations, such as wind and solar, are increasingly installed into electric power grids all over the world in an effort to reduce CO<sub>2</sub> emissions from the electricity generation sector. Yet, their natural intermittency presents major challenges to the delivery of consistent power that is necessary for today’s grid operation, in which generation must be adjusted to meet load. Also, the inherently low inertia of renewable generators limits the grid’s controllability and makes the grid easy to lose its stability. The existing power grids and management tools are not designed to deal with these new challenges. Therefore, new stability assessment and control design tools are needed to adapt with the shift in architecture and dynamic behavior of future grids.

Transient stability assessment of power system certifies if the system converges to a stable operating condition after experiencing large disturbances. Traditionally, this task is handled by using either time domain simulation [1], or by utilizing direct energy method and Lyapunov function method [2]–[6] to estimate the stability region of a given equilibrium point (EP), i.e., the set of initial states from which power system will converge to that EP. In modern renewable power grids, the operating point is constantly moving in an unpredictable way because of the real-time clearing of electricity markets, intermittent renewable generations, changing loads, and external disturbances. The constant changing of the EP makes the transient stability assessment even more technically difficult and computationally cumbersome.

All authors are with Massachusetts Institute of Technology, Cambridge, MA 02139, USA, email: {longvu, hunghtd, ameg, jjs, turitsyn}@mit.edu.

In this letter, rather than considering the stability assessment, we formulate the *inverse stability assessment problem*. This problem concerns with estimating the region around a given initial state, called “*inverse stability region*”, such that whenever power injections or power lines change and the resulting EP stays in this region, then power system will converge from the given initial state to the EP. Indeed, such convergence is guaranteed when the system’s energy function is bounded under some threshold [2], [3]. In [7], we observed that if the EP stays strictly inside polytope  $\mathcal{P}$  characterized by phasor angular differences smaller than  $\pi/2$ , then the nonlinear power flows can be strictly bounded by linear functions of angular differences. Exploiting this observation, we show that the energy function of power system can be bounded by quadratic functions of the EP and the system state, and thereby we obtain an estimate of the inverse stability region.

The remarkable advantage of the inverse stability certificate is allowing us to analyze and exploit the change of EP to achieve useful dynamical properties. We will briefly discuss three applications of this certificate, that are of importance to the integration of large-scale renewable generations:

**Robust stability assessment:** For a typical power system composed of tens to hundred thousands of components, there are millions of contingencies that need to be reassessed on a regular basis. Most of these contingencies correspond to failures of relatively small and insignificant components, so the post-contingency states are close to the stable EP and the post-fault dynamics is probably transiently stable. Therefore, most of the computational effort is spent on the analysis of non-critical scenarios. This computational burden could be greatly alleviated by a robust transient stability assessment toolbox that could certify stability of power systems with broad range of uncertainties. In this letter, we show that the inverse stability certificate can be employed to assess the transient stability of power systems when there is fluctuation in power injections from renewable generations.

**Stability-constrained OPF:** Under large disturbances, the stressed power systems with the normal operating condition, which is derived by solving conventional OPF problem, may not survive. It is therefore desirable to design operating conditions that can withstand large disturbances. This can be carried out by incorporating transient stability constraint into OPF together with the normal voltage and thermal constraints. Though this problem was discussed in the literature, there is

no way to precisely formulate and solve the stability-constrained OPF problem because transient stability is a dynamic concept and differential equations are involved in stability constraint, which together make the sOPF computationally intractable by the existing optimization methods. *Fortunately, the inverse stability certificate essentially transforms the dynamic problem of trajectory convergence into the static problem of placing the EP into a prescribed set, which is much more computationally tractable.* Indeed, this naturally allows for the integration of transient stability constraint as a static constraint into the standard OPF problem.

**Stability-guaranteed corrective actions:** Traditional protection strategies for power systems focus on the safety of individual components, and the level of coordination among component protection systems is far from perfect. Also, the existing special protection systems do not take full advantage of the new flexible and fast electronics resources available in modern power systems, and largely rely on customer-harmful actions like load shedding. These considerations motivated us to exploit flexible electronics resources to relocate the operating point as a system-level corrective action with guaranteed stability [8]. This letter shows that we can appropriately redispatch power injections to relocate the EP as desired (i.e., staying near the emergency state) and stabilize power systems under emergency situations. The inverse stability certificate will help us accurately design a sequence of EPs such that the convergence of the system from the emergency state through the sequence of EPs to desired place is guaranteed.

In this letter, we aim at introducing relevant power engineering problems to control community, and thus, we mainly focus on discussing the applications of the inverse stability certificate to the OPF, stability analysis and control problems. More complete solutions to these problems can be obtained by combining with other techniques and approaches well developed in the literature.

In overall, the contributions of this paper are as follows:

- We formulate, for the first time, the inverse stability problem of power systems and introduce an inverse stability certificate.
- We apply this certificate to relocate the EP by suitably dispatching the power injections such that power system is driven to stability regime under emergency situations.
- We show that this certificate can be applied to assess the stability of renewable power system and to effectively solve the open problem of stability-constrained OPF.

## II. INVERSE STABILITY PROBLEM OF POWER SYSTEMS

In this letter, we utilize the standard structure-preserving model to describe the post-fault dynamics of power systems consisting of generators and loads [9]. This model naturally incorporates the dynamics of the generators' rotor angle as well as the response of load power output to frequency deviation. Mathematically, the grid is described by an undirected graph  $\mathcal{A}(\mathcal{N}, \mathcal{E})$ , where  $\mathcal{N} = \{1, 2, \dots, |\mathcal{N}|\}$  is the set of

buses and  $\mathcal{E} \subseteq \mathcal{N} \times \mathcal{N}$  is the set of transmission lines connecting those buses. Here,  $|A|$  denotes the number of elements in set  $A$ . The sets of generator buses and load buses are denoted by  $\mathcal{G}$  and  $\mathcal{L}$ . We assume that the grid is lossless with constant voltage magnitudes  $V_k, k \in \mathcal{N}$ , and the reactive powers are ignored. Then, the structure-preserving model of the system is given by [9]:

$$m_k \ddot{\delta}_k + d_k \dot{\delta}_k + \sum_{j \in \mathcal{N}_k} a_{kj} \sin(\delta_k - \delta_j) = P_k, k \in \mathcal{G}, \quad (1a)$$

$$d_k \dot{\delta}_k + \sum_{j \in \mathcal{N}_k} a_{kj} \sin(\delta_k - \delta_j) = P_k, k \in \mathcal{L}, \quad (1b)$$

where equation (1a) represents the dynamics at generator buses and equation (1b) the dynamics at load buses. Here,  $a_{kj} = V_k V_j B_{kj}$ , where  $B_{kj}$  is the (normalized) susceptance of the transmission line  $\{k, j\}$  connecting the  $k^{th}$  bus and  $j^{th}$  bus.  $\mathcal{N}_k$  is the set of neighboring buses of the  $k^{th}$  bus (see [10] for more details).

In normal conditions, a power grid operates at an operating condition of the *pre-fault dynamics*. Under the fault, the system evolves according to the *fault-on dynamics*. After some time period, the fault is cleared or self-clears, and the system is at the so-called *fault-cleared state*  $\delta_0$ . Then, the power system experiences the so-called *post-fault dynamics*. The transient stability assessment problem addresses the question of whether the post-fault dynamics converges from the fault-cleared state  $\delta_0$  to a post-fault stable EP  $\delta^*$ . Mathematically, this operating condition, characterized by the angles  $\delta_k^*$ , is not unique since any uniform shift of the angles  $\delta_k^* \rightarrow \delta_k^* + c$  is also an equilibrium of (1a)-(1b). However, it is unambiguously characterized by the angle differences  $\delta_{kj}^* = \delta_k^* - \delta_j^*$  that solve the following system of power-flow like equations:

$$\sum_{j \in \mathcal{N}_k} a_{kj} \sin \delta_{kj} = P_k, k \in \mathcal{N}. \quad (2)$$

When the power injections  $P_k$  fluctuate and/or the couplings  $a_{kj}$  vary, then the resulting EP  $\delta^*$  also fluctuates. Therefore, we want to characterize the region of EPs such that the post-fault dynamics always converge from a given initial state  $\delta_0$  to the EP whenever the EP belongs to this region. Formally, we consider the inverse stability problem:

- **Inverse Stability Problem:** Consider a given initial state  $\delta_0$ . Assume that power injections fluctuate, and that the line susceptances vary such that  $\bar{a}_{kj} \geq a_{kj} \geq \underline{a}_{kj}$ . Estimate the region of stable EPs of the system (1) such that the system always converges from  $\delta_0$  to the EP whenever the EP stays inside this region.

This problem will be solved with the inverse stability certificate to be presented in the next section by exploiting quadratic bounds of the system's energy function.

## III. ENERGY FUNCTION AND INVERSE STABILITY CERTIFICATE

### A. Stability assessment by using energy function

For the structure-preserving model (1), we consider the energy function which characterizes how far is it from the

state  $\delta$  to the EP  $\delta^*$  :

$$E = \sum_{k \in \mathcal{G}} \frac{m_k \dot{\delta}_k^2}{2} + \sum_{\{k,j\} \in \mathcal{E}} \int_{\delta_{kj}^*}^{\delta_{kj}} a_{kj} (\sin \xi - \sin \delta_{kj}^*) d\xi \quad (3)$$

Then, along the trajectory of (1), we have

$$\begin{aligned} \dot{E} &= \sum_{k \in \mathcal{G}} m_k \dot{\delta}_k \ddot{\delta}_k + \sum_{\{k,j\} \in \mathcal{E}} a_{kj} (\sin \delta_{kj} - \sin \delta_{kj}^*) \dot{\delta}_{kj} \\ &= \sum_{k \in \mathcal{G}} \dot{\delta}_k (P_k - d_k \dot{\delta}_k - \sum_{j \in \mathcal{N}_k} a_{kj} \sin(\delta_k - \delta_j)) \\ &+ \sum_{k \in \mathcal{L}} \dot{\delta}_k (P_k - d_k \dot{\delta}_k - \sum_{j \in \mathcal{N}_k} a_{kj} \sin(\delta_k - \delta_j)) \\ &+ \sum_{\{k,j\} \in \mathcal{E}} a_{kj} (\sin \delta_{kj} - \sin \delta_{kj}^*) (\dot{\delta}_k - \dot{\delta}_j) \\ &= - \sum_{k \in \mathcal{N}} d_k (\dot{\delta}_k)^2 \leq 0, \end{aligned} \quad (4)$$

in which the last equation is obtained from the power flow-like equations,  $P_k = \sum_{j \in \mathcal{N}_k} a_{kj} \sin \delta_{kj}^*$ , for all  $k \in \mathcal{N}$ . Hence, the energy function  $E(\delta, \delta^*)$  is always decreasing (but not strictly decreasing) along the trajectory of (1).

Consider the polytope  $\mathcal{P}$  defined by inequalities  $|\delta_{kj}| \leq \pi/2, \forall \{k, j\} \in \mathcal{E}$ . Then,  $E(\delta, \delta^*) \geq 0, \forall \delta, \delta^* \in \mathcal{P}$ . Hence, the energy function is lower bounded by 0 when the system state staying inside polytope  $\mathcal{P}$ . By using LaSalle Invariant Principle and similar proof with that of Theorem 1 in [7], we can show that if the initial state  $\delta_0$  stays inside the set  $\{\delta \in \mathcal{P} : E(\delta, \delta^*) < \min_{\delta \in \partial \mathcal{P}} E(\delta, \delta^*)\}$ , then the system will only evolve inside this set and eventually converge to the equilibrium point  $\delta^*$ . So, to check if the system converges from  $\delta_0 \in \mathcal{P}$  to the EP  $[\delta^* \ 0]^\top$ , we only need to check if  $E(\delta_0, \delta^*) < E_{\min}$  where  $E_{\min} = \min_{\delta \in \partial \mathcal{P}} E(\delta, \delta^*)$ .

### B. Inverse stability certificate

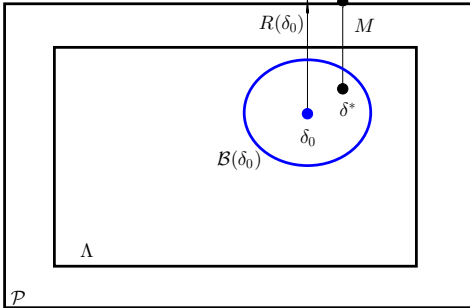


Fig. 1. For a power system with a given initial state  $[\delta_0 \ \dot{\delta}_0]^\top$ , whenever the EP  $[\delta^* \ 0]^\top$  stays inside the set  $\Lambda \cap \mathcal{B}(\delta_0)$  surrounding  $\delta_0$ , then the power system will converge from  $\delta_0$  to the EP since  $E(\delta_0, \delta^*) < E_{\min}$ .

To establish the inverse stability certificate, we combine the above stability analysis with quadratic bounds of the energy function  $E(\delta, \delta^*)$  for any  $\delta^*$  stays in the polytope  $\Lambda$  defined by inequalities  $|\delta_{kj}| \leq \lambda < \pi/2, \forall \{k, j\} \in \mathcal{E}$ . Let

$$g = \frac{1 - \sin \lambda}{\pi/2 - \lambda} > 0. \text{ In [7], we observed that}$$

$$g(\xi - \delta_{kj}^*)^2 \leq (\xi - \delta_{kj}^*) (\sin \xi - \sin \delta_{kj}^*) \leq (\xi - \delta_{kj}^*)^2,$$

for any  $|\xi| \leq \pi/2$  and  $|\delta_{kj}^*| \leq \lambda$ . As such, if the EP  $\delta^*$  stays in polytope  $\Lambda$  and the state  $\delta$  stays in polytope  $\mathcal{P}$ , then

$$\begin{aligned} E(\delta, \delta^*) &\geq \sum_{k \in \mathcal{G}} \frac{m_k \dot{\delta}_k^2}{2} + \sum_{\{k,j\} \in \mathcal{E}} \int_{\delta_{kj}^*}^{\delta_{kj}} a_{kj} g(\xi - \delta_{kj}^*) d\xi \\ &= \sum_{k \in \mathcal{G}} \frac{m_k \dot{\delta}_k^2}{2} + g \sum_{\{k,j\} \in \mathcal{E}} a_{kj} \frac{(\delta_{kj} - \delta_{kj}^*)^2}{2} \end{aligned} \quad (5)$$

Similarly, for all  $\delta^* \in \Lambda, \delta \in \mathcal{P}$ , we have

$$E(\delta, \delta^*) \leq \sum_{k \in \mathcal{G}} \frac{m_k \dot{\delta}_k^2}{2} + \sum_{\{k,j\} \in \mathcal{E}} a_{kj} \frac{(\delta_{kj} - \delta_{kj}^*)^2}{2} \quad (6)$$

Define the following quadratic functions

$$D(\delta, \delta^*) = g \sum_{\{k,j\} \in \mathcal{E}} \underline{a}_{kj} \frac{(\delta_{kj} - \delta_{kj}^*)^2}{2}, \quad (7)$$

$$F(\delta, \delta^*) = \sum_{k \in \mathcal{G}} \frac{m_k \dot{\delta}_k^2}{2} + \sum_{\{k,j\} \in \mathcal{E}} \bar{a}_{kj} \frac{(\delta_{kj} - \delta_{kj}^*)^2}{2}.$$

From (5) and (6), we can bound the energy function as

$$D(\delta, \delta^*) \leq E(\delta, \delta^*) \leq F(\delta, \delta^*), \forall \delta \in \mathcal{P}, \delta^* \in \Lambda. \quad (8)$$

For a given initial state  $[\delta_0 \ \dot{\delta}_0]^\top$  staying inside polytope  $\mathcal{P}$ , we calculate the “distance” from this initial state to the boundary of polytope  $\mathcal{P}$  :  $R(\delta_0) = \min_{\delta \in \partial \mathcal{P}} D(\delta_0, \delta)$ . Define the set surrounding the initial state  $\delta_0$  :

$$\mathcal{B}(\delta_0) = \{(\delta, \dot{\delta}) : F(\delta_0, \delta) \leq R(\delta_0)/4\}. \quad (9)$$

We have the following center result regarding the inverse stability of power system, as depicted in Fig. 1.

*Theorem 1:* Consider a given initial state  $[\delta_0 \ \dot{\delta}_0]^\top$  staying inside polytope  $\mathcal{P}$ . Assume that the EP of the system varies due to the fluctuation in power injections or line susceptances, but it stays inside the set  $\Lambda \cap \mathcal{B}(\delta_0)$ , where the set  $\mathcal{B}(\delta_0)$  is defined as in (9). Then, the system always converges from the given initial state  $\delta_0$  to the (varying) EP.

*Proof:* See Appendix VI.  $\square$

We note that the above inverse stability certificate is applicable to both cases when the EP varies due to the fluctuations of power injections and transmission line susceptances. If we only consider the fluctuation of power injections, then the above results hold true with  $\bar{a}_{kj}$  and  $\underline{a}_{kj}$  in Eqs. (7) replaced by  $a_{kj}$ . Such flexibility will be exploited in several applications to be discussed in the next section.

## IV. APPLICATIONS OF INVERSE STABILITY CERTIFICATE

### A. Robust stability assessment

The robust transient stability problem that we consider involves situations where there is uncertainty in power injections  $P_k$ , the sources of which can be intermittent renewable generations. Formally, for a given fault-cleared state  $\delta_0$ , we need to certify the transient stability of the post-fault dynamics described by (1) with respect to the fluctuation of the power injections, which consequently leads to the varying of the post-fault EP  $\delta^*$  obtained from solving the

power flow equations (2). Therefore, we concern with the following robust stability problem [7]:

- **Robust stability assessment:** *Given a fault-cleared state  $\delta_0$ , certify the transient stability of (1) w.r.t. a set of stable EPs  $\delta^*$  resulted from the fluctuation of renewable generations.*

Utilizing the inverse stability certificate, we can make sure the robust stability of renewable power systems whenever the resulting EP stays inside the set  $\Lambda \cap \mathcal{B}(\delta_0)$ . To check if the EP stays in polytope  $\Lambda$ , we can apply the criterion in [11], which states that the EP almost surely stays in polytope  $\Lambda$  if the power injections  $p = [P_1, \dots, P_{|\mathcal{N}|}]^T$  satisfies

$$\|L^\dagger p\|_{\mathcal{E}, \infty} \leq \sin \lambda, \quad (10)$$

where  $L^\dagger$  is the pseudoinverse of the network Laplacian matrix and the norm  $\|x\|_{\mathcal{E}, \infty}$  is defined as  $\|x\|_{\mathcal{E}, \infty} = \max_{\{i,j\} \in \mathcal{E}} |x(i) - x(j)|$ . On the other hand, some possible bound for the relation between the EP and the power injection vector  $p$  can be established, in the similar way with that in [11], such that we can verify if the EP stays in the set  $\mathcal{B}(\delta_0)$  through checking the power injections  $p$ .

### B. Stability-constrained OPF

Stability-constrained OPF problem concerns with determining the optimal operating condition in the respect to voltage and thermal constraints as well as stability constraint. While voltage and thermal constraints are well modeled via algebraic equations or inequalities, it is still an open question as to how to include stability constraint into OPF formulation since stability is a dynamic concept and differential equations are involved. Even when the problem is relaxed, it is computationally hard to get a solution of a stability-constrained OPF problem since the stability constraint have to be approximated and updated in each step of solving OPF in conventional approaches [12].

Mathematically, a standard OPF problem is as follows:

$$\min c(p) \quad (11)$$

$$s.t. \quad P(V, \delta) = P \quad (12)$$

$$Q(V, \delta) = Q \quad (13)$$

$$\underline{V} \leq V \leq \bar{V} \quad (14)$$

$$\underline{S} \leq |S(V, \delta)| \leq \bar{S} \quad (15)$$

where  $c(p)$  is a cost function, the equality constraints (12)-(13) stand for the power flow equations, and the inequality constraints (14)-(15) stand for the voltage and thermal limits of branch flows through transmission lines and transformers. Assume that the stability constraint is to make sure that the system will converge from a given fault-cleared state  $\delta_0$  to the designed operating condition, and that the reactive power is negligible. With the inverse stability certificate, the stability constraint can be relaxed and formulated as  $\delta \in \Lambda \cap \mathcal{B}(\delta_0)$ . Basically, the inverse stability certificate transforms the dynamic problem of convergence guaranteeing into a static, computationally tractable problem of placing the prospective EP into a prescribed set. In summary, we obtain the stability-constrained OPF formulation:

$$\min c(p) \quad (16)$$

$$s.t. \quad P(V, \delta) = P \quad (17)$$

$$\underline{V} \leq V \leq \bar{V} \quad (18)$$

$$\underline{S} \leq |S(V, \delta)| \leq \bar{S} \quad (19)$$

$$\delta \in \Lambda \cap \mathcal{B}(\delta_0). \quad (20)$$

Solving this optimization problem, we obtain an operating condition at which the cost function is minimized and the voltage/thermal constraints are respected. Furthermore, the stability constraint is guaranteed by the inverse stability certificate, and the system is ensured to converge from the fault-cleared  $\delta_0$  to the obtained operating condition.

### C. Emergency control design

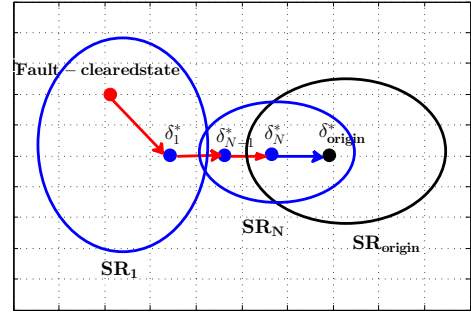


Fig. 2. Power dispatching to relocate the stable EPs  $\delta_i^*$  such that the fault-cleared state, which is possibly unstable if there is no controls, is driven through the sequence of EPs back to the desired EP  $\delta_{\text{origin}}^*$ . The placement of the EP is determined by applying the inverse stability certificate.

Another application of the inverse stability certificate, that will be detailed in this section, is designing the stability-guaranteed corrective actions that can drive the post-fault dynamics to a stability regime. When the fault-cleared state is given, by applying the inverse stability certificate, we can appropriately dispatch the power injections  $P_k$  to relocate the EP of the system such that the post-fault dynamics can be attracted from the fault-cleared state  $\delta_0$  through a sequence of EPs to the original EP  $\delta_{\text{origin}}^*$ , as illustrated in Fig. 2. This type of corrective actions will alleviate load shedding and state measurement, as well as requiring minor investment since it can be implemented by FACTS devices being increasingly installed into transmission networks.

Mathematically, we consider the following problem:

- **Emergency Control Design:** *Given a fault-cleared state  $\delta_0$  and the stable EP  $\delta_{\text{origin}}^*$ , determine the feasible dispatching of power injections  $P_k$  to relocate the EPs such that the post-fault dynamics is driven from the fault-cleared state  $\delta_0$  through the set of designed EPs to the desired post-fault EP  $\delta_{\text{origin}}^*$ .*

To solve this problem, we can design the first EP  $\delta_1^*$  by minimizing  $\|L^\dagger p\|_{\mathcal{E}, \infty}$  over all possible power injections. The optimum power injection will result in an EP which is most far away from the stability margin  $|\delta_{kj}| = \pi/2$ , and hence, the stability region of the first EP  $\delta_1^*$  probably contains

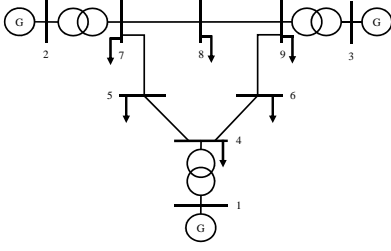


Fig. 3. 3-generator 9-bus system with frequency-dependent dynamic loads.

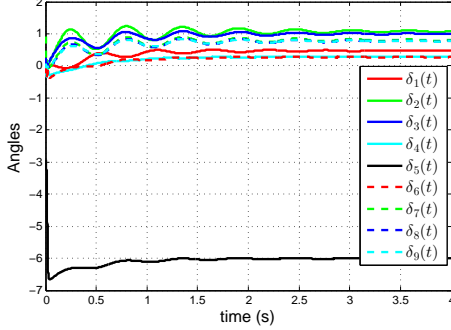


Fig. 4. Unstable post-fault dynamics when there is no controls:  $|\delta_{45}|$  and  $|\delta_{57}|$  evolve to  $2\pi$ , triggering the tripping of lines  $\{4, 5\}$  and  $\{5, 7\}$ .

the given fault-cleared state. To design the sequence of EPs, in each step, we carry out the following tasks:

- Calculate the distance  $R(\delta_{i-1}^*)$  from the given EP  $\delta_{i-1}^*$  to the boundary of polytope  $\mathcal{P}$ , i.e.,  $R(\delta_{i-1}^*) = \min_{\delta \in \partial \mathcal{P}} D(\delta, \delta_{i-1}^*)$ . Noting that minimization of  $D(\delta, \delta_{i-1}^*)$  over the boundary of polytope  $\mathcal{P}$  is a convex problem with quadratic objective function and linear constraints. Hence, we can quickly obtain  $R(\delta_{i-1}^*)$ .
- Determine the set  $\mathcal{B}(\delta_{i-1}^*)$  and the set  $\Lambda \cap \mathcal{B}(\delta_{i-1}^*)$ .
- The next EP  $\delta_i^*$  will be chosen as the intersection of the boundary of the set  $\Lambda \cap \mathcal{B}(\delta_{i-1}^*)$  and the line segment connecting  $\delta_{i-1}^*$  and  $\delta_{\text{origin}}^*$ .
- The power injections  $P_k$  that we have to redispatch will be determined by  $P_k^{(i)} = \sum_{j \in \mathcal{N}_k} a_{kj} \sin \delta_{i,j}^*$  for all  $k$ . This power dispatch will place the new EP at  $\delta_i^*$  which stays in the inverse stability region of the previous EP  $\delta_{i-1}^*$ . Therefore, the controlled post-fault dynamics will converge from  $\delta_{i-1}^*$  to  $\delta_i^*$ .

This procedure strictly reduces the distance from EP to  $\delta_{\text{origin}}^*$ . Hence, after some steps, the EP  $\delta_N^*$  will be sufficiently near the desired EP  $\delta_{\text{origin}}^*$  such that the convergence of the system to the desired EP  $\delta_{\text{origin}}^*$  will be guaranteed.

To illustrate that this control works well in stabilizing some possibly unstable fault-cleared state  $\delta_0$ , we consider the 3-machine 9-bus system with 3 generator buses and 6 frequency-dependent load buses as in Fig. 3. The susceptances of the transmission lines are as follows:  $B_{14} = 17.3611 p.u.$ ,  $B_{27} = 16.0000 p.u.$ ,  $B_{39} = 17.0648 p.u.$ ,  $B_{45} = 11.7647 p.u.$ ,  $B_{57} = 6.2112 p.u.$ ,  $B_{64} = 10.8696 p.u.$ ,  $B_{78} = 13.8889 p.u.$ ,  $B_{89} = 9.9206 p.u.$ ,  $B_{96} = 5.8824 p.u.$  The parameters for generators are:  $m_1 = 0.1254$ ,  $m_2 = 0.034$ ,  $m_3 = 0.016$ ,  $d_1 = 0.0627$ ,  $d_2 =$

Node	V (p.u.)	$P_k$ (p.u.)
1	1.0284	3.6466
2	1.0085	4.5735
3	0.9522	3.8173
4	1.0627	-3.4771
5	1.0707	-3.5798
6	1.0749	-3.3112
7	1.0490	-0.5639
8	1.0579	-0.5000
9	1.0521	-0.6054

TABLE I

BUS VOLTAGES, MECHANICAL INPUTS, AND STATIC LOADS.

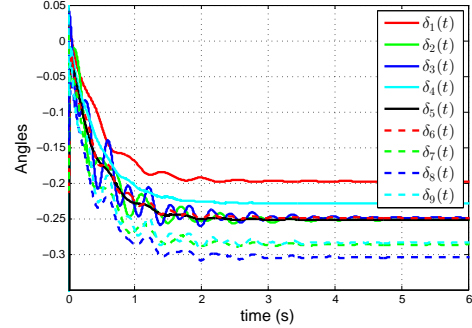


Fig. 5. Stable dynamics with power injection control: Convergence of buses angles from the fault-cleared state to  $\delta_1^*$  in the post-fault dynamics

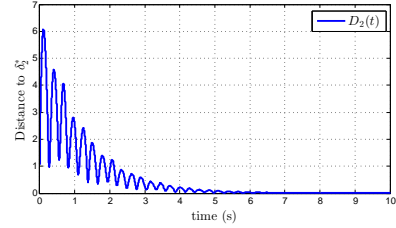


Fig. 6. Effect of power dispatching control: the convergence of the distance  $D_2(t)$  to 0. Here, the Euclid distance  $D_2(t)$  between a state  $\delta$  and the second EP  $\delta_2^*$  is defined as  $D_2(t) = \sqrt{\sum_{i=2}^9 (\delta_{i1}(t) - \delta_{i1}^*)^2}$ .

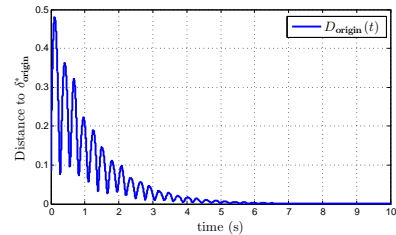


Fig. 7. Autonomous dynamics when we switch the power injections to the originally preferred values: the convergence of the distance  $D_{\text{origin}}(t)$  to 0. Here, the distance  $D_{\text{origin}}(t)$  between a state  $\delta$  and the original EP  $\delta_{\text{origin}}^*$  is defined as  $D_{\text{origin}}(t) = \sqrt{\sum_{i=2}^9 (\delta_{i1}(t) - \delta_{\text{origin},i1}^*)^2}$ .

$0.017$ ,  $d_3 = 0.008$ . For simplicity, we take  $d_k = 0.05$ ,  $k = 4 \dots, 9$ . Assume that the fault trips the line between buses 5 and 7, and make the power injections to fluctuate. When the fault is cleared this line is re-closed. We also assume the fluctuation of the generation (probably due to renewables) and load such that the bus voltages  $V_k$  and power injections

$P_k$  of the post-fault dynamics after clearing the fault are given in Tab. I. The stable operating condition is calculated as  $\delta_{\text{origin}}^* = [-0.1629 \ 0.4416 \ 0.3623 \ -0.3563 \ -0.3608 \ -0.3651 \ 0.1680 \ 0.1362 \ 0.1371]^\top$ ,  $\dot{\delta}_{\text{origin}}^* = 0$ . However, the fault-cleared state, with angles  $\delta_0 = [0.025 \ -0.023 \ 0.041 \ 0.012 \ -2.917 \ -0.004 \ 0.907 \ 0.021 \ 0.023]^\top$  and generators angular velocity  $[-0.016 \ -0.021 \ 0.014]^\top$ , stays outside polytope  $\mathcal{P}$ . It can be seen from Fig. 4 that the uncontrolled post-fault dynamics is not stable since  $|\delta_{45}|$  and  $|\delta_{57}|$  quickly evolve from initial values to  $2\pi$ , which will activate the protective devices to trip the lines.

Using CVX software to minimize  $\|L^\dagger p\|_{\mathcal{E},\infty}$ , we obtain the new power injections at buses 1-6 as follows:  $P_1 = 0.5890, P_2 = 0.5930, P_3 = 0.5989, P_4 = -0.0333, P_5 = -0.0617$ , and  $P_6 = -0.0165$ . Accordingly, the minimum value of  $\|L^\dagger p\|_{\mathcal{E},\infty} = 0.0350 < \sin(\pi/89)$ . Hence, the first EP obtained from equation (2) will stay in the polytope defined by the inequalities  $|\delta_{kj}| \leq \pi/89, \forall \{k, j\} \in \mathcal{E}$ , and can be approximated by  $\delta_1^* \approx L^\dagger p = [0.0581 \ 0.0042 \ 0.0070 \ 0.0271 \ 0.0042 \ 0.0070 \ -0.0308 \ -0.0486 \ -0.0281]^\top$ . The simulation results confirm that the post-fault dynamics is made stable by applying the optimum power injection control, as showed in Fig. 5. Using the above procedure, after one step, we can find that  $\delta_2^* = 0.9259\delta_{\text{origin}}^* + 0.0741\delta_1^*$  is the intersection of the set  $\Lambda \cap \mathcal{B}(\delta_1^*)$  and the line segment connecting  $\delta_1^*$  and  $\delta_{\text{origin}}^*$ . This EP stays inside the inverse stability region of  $\delta_1^*$ , and hence the system will converge from  $\delta_1^*$  to  $\delta_2^*$  when we do the power dispatching  $P_k^{(2)}$  corresponding to  $\delta_2^*$ . On the other hand,  $\delta_2^*$  is very near the desired EP  $\delta_{\text{origin}}^*$  and it is easy to check that  $\delta_{\text{origin}}^*$  stays in the inverse stability region of  $\delta_2^*$ , and thus the system will converge from  $\delta_2^*$  to the desired EP  $\delta_{\text{origin}}^*$ . Such convergence of the controlled post-fault dynamics is confirmed in Figs. 6-7.

## V. CONCLUSIONS

Power grids possess many distinguished dynamical properties, e.g. prohibition of global stability and exhibition of significant uncertainties, that challenge the maintenance of their reliable operation and pose interesting questions to control and power communities. In this letter, we characterized a surprising property, namely ‘‘inverse stability’’, which was rarely investigated. By exploiting the quadratic lower bound of energy function, we introduced an inverse stability certificate, which gave us an estimate of the region of EPs around a given initial state such that, whenever the EP changes (due to the fluctuation in power injections/line susceptances) but stays in this region, then power system will converge from the initial state to the EP. In addition, we briefly described three applications of this certificate: (i) assessing the stability of renewable power systems, (ii) facilitating stability-constrained OPF, and (iii) designing power dispatching remedial action to recover the transient stability of power systems. Remarkably, we showed that robust stability due to the fluctuation of renewable generations can be effectively assessed, and that stability constraint can be conveniently incorporated into a computationally tractable

OPF problem. We also illustrated that the proposed corrective action can drive a given fault-cleared state, that originally leads to unstable dynamics, to the desired stable EP.

## VI. APPENDIX: PROOF OF THEOREM 1

For each EP  $\delta^* \in \Lambda \cap \mathcal{B}(\delta_0)$ , let  $M$  be the point on the boundary of polytope  $\mathcal{P}$  such that  $E(M, \delta^*) = E_{\min}(\delta^*) = \min_{\delta \in \partial \mathcal{P}} E(\delta, \delta^*)$ , as depicted in Fig. 1. From (8), we have

$$\begin{aligned} E(M, \delta^*) + E(\delta_0, \delta^*) &\geq D(M, \delta^*) + D(\delta_0, \delta^*) \\ &= g \sum_{\{k,j\} \in \mathcal{E}} \frac{a_{kj} (\delta_{Mkj} - \delta_{kj}^*)^2 + (\delta_{0kj} - \delta_{kj}^*)^2}{2} \\ &\geq g \sum_{\{k,j\} \in \mathcal{E}} \frac{a_{kj} (\delta_{Mkj} - \delta_{0kj})^2}{4} = \frac{D(\delta_0, M)}{2}. \end{aligned} \quad (21)$$

Note that  $D(\delta_0, M) \geq R(\delta_0)$  as  $R(\delta_0)$  is the distance from  $\delta_0$  to the boundary of polytope  $\mathcal{P}$ . This, together with (21), leads to  $E(M, \delta^*) + E(\delta_0, \delta^*) \geq R(\delta_0)/2$ . From (8) and (9), we have  $E(\delta_0, \delta^*) \leq F(\delta_0, \delta^*) < R(\delta_0)/4$ . Hence,

$$E(M, \delta^*) > R(\delta_0)/4 > E(\delta_0, \delta^*). \quad (22)$$

Therefore, for any  $\delta^* \in \Lambda \cap \mathcal{B}(\delta_0)$ , we have  $E(\delta_0, \delta^*) < E_{\min}(\delta^*)$ . By analysis in Section III-A, the initial state  $\delta_0$  must stay inside the stability region of the EP  $\delta^*$  and the system will converge from the initial state  $\delta_0$  to the EP  $\delta^*$ .

## REFERENCES

- [1] I. Nagel, L. Fabre, M. Pastre, F. Krummenacher, R. Cherkaoui, and M. Kayal, ‘‘High-Speed Power System Transient Stability Simulation Using Highly Dedicated Hardware,’’ *Power Systems, IEEE Transactions on*, vol. 28, no. 4, pp. 4218–4227, 2013.
- [2] M. A. Pai, K. R. Padiyar, and C. RadhaKrishna, ‘‘Transient Stability Analysis of Multi-Machine AC/DC Power Systems via Energy-Function Method,’’ *Power Engineering Review, IEEE*, no. 12, pp. 49–50, 1981.
- [3] H.-D. Chiang, *Direct Methods for Stability Analysis of Electric Power Systems*, ser. Theoretical Foundation, BCU Methodologies, and Applications. Hoboken, NJ, USA: John Wiley & Sons, Mar. 2011.
- [4] H.-D. Chiang, F. F. Wu, and P. P. Varaiya, ‘‘A BCU method for direct analysis of power system transient stability,’’ *Power Systems, IEEE Transactions on*, vol. 9, no. 3, pp. 1194–1208, Aug. 1994.
- [5] D. J. Hill and C. N. Chong, ‘‘Lyapunov functions of Lur’e-Postnikov form for structure preserving models of power systems,’’ *Automatica*, vol. 25, no. 3, pp. 453–460, May 1989.
- [6] R. Davy and I. A. Hiskens, ‘‘Lyapunov functions for multi-machine power systems with dynamic loads,’’ *Circuits and Systems I: Fundamental Theory and Applications, IEEE Transactions on*, vol. 44, no. 9, pp. 796–812, 1997.
- [7] T. L. Vu and K. Turitsyn, ‘‘A framework for robust assessment of power grid stability and resiliency,’’ *IEEE Transactions on Automatic Control*, vol. PP, no. 99, pp. 1–1, 2016.
- [8] T. L. Vu, S. Chatzivasileiadis, H. D. Chiang, and K. Turitsyn, ‘‘Structural emergency control paradigm,’’ *IEEE Journal on Emerging and Selected Topics in Circuits and Systems*, vol. PP, no. 99, pp. 1–12, 2017.
- [9] A. R. Bergen and D. J. Hill, ‘‘A structure preserving model for power system stability analysis,’’ *Power Apparatus and Systems, IEEE Transactions on*, no. 1, pp. 25–35, 1981.
- [10] T. L. Vu, S. M. A. Arafi, M. S. E. Moursi, and K. Turitsyn, ‘‘Toward simulation-free estimation of critical clearing time,’’ *IEEE Transactions on Power Systems*, vol. PP, no. 99, pp. 1–10, 2016.
- [11] F. Dorfler, M. Chertkov, and F. Bullo, ‘‘Synchronization in complex oscillator networks and smart grids,’’ *Proceedings of the National Academy of Sciences*, vol. 110, no. 6, pp. 2005–2010, 2013.
- [12] D. Gan, R. J. Thomas, and R. D. Zimmerman, ‘‘Stability-constrained optimal power flow,’’ *IEEE Transactions on Power Systems*, vol. 15, no. 2, pp. 535–540, May 2000.